

# Feasibility Study of Developing Green ECC Using Iron Ore Tailings Powder as Cement Replacement

Xiaoyan Huang<sup>1</sup>; Ravi Ranade<sup>2</sup>; and Victor C. Li, F.ASCE<sup>3</sup>

**Abstract:** This paper reports the results of an initial attempt of using iron ore tailings (IOTs) to develop greener engineered cementitious composites (ECCs). ECC is a unique class of high-performance fiber-reinforced cementitious composites featuring high tensile ductility and durability. However, the high cement usage in ECC limits the material greenness and increases the material cost compared with normal concrete. In this paper, IOTs in powder form are used to partially replace cement to enhance the environmental sustainability of ECC. Mechanical properties and material greenness of ECC containing various proportions of IOTs are investigated. The newly developed versions of ECC in this paper, with a cement content of 117.2–350.2 kg/m<sup>3</sup>, exhibit a tensile ductility of 2.3–3.3%, tensile strength of 5.1–6.0 MPa, and compressive strength of 46–57 MPa at 28 days. The replacement of cement with IOTs results in 10–32% reduction in energy consumption and 29–63% reduction in carbon dioxide emissions in green ECC compared with typical ECC. Thus, the feasibility of producing greener ECC with significantly reduced environmental impact using IOTs, and maintaining the mechanical properties of typical ECC, is experimentally demonstrated in this paper. DOI: 10.1061/(ASCE)MT.1943-5533.0000674. © 2013 American Society of Civil Engineers.

**CE Database subject headings:** Cement; Composite materials; Sustainable development; Ductility; Tailings.

**Author keywords:** Engineered cementitious composites; Sustainability; Tensile ductility; Iron ore tailings.

## Introduction

Iron ore tailings (IOTs) are large piles of ground rocks that are discarded during the beneficiation process of iron ore concentration. In rapidly developing countries like China, the generation of IOTs has been increasing rapidly as a result of the growing demand of iron and steel in recent years. For instance, the annual generation of IOTs increased from 137 billion kg in 2000 to 536 billion kg in 2009, and the total accumulation of IOTs from 2000–2009 exceeded 2.8 trillion kg (Meng et al. 2011). In spite of such a huge amount of IOTs stockpiled as waste, the current utilization rate of IOTs in China is less than 10% [Ministry of Industry and Information Technology of the People's Republic of China (MIITPRC) 2013]. Such underutilization of a natural resource (i.e., IOTs) not only places a heavy economic burden of waste management on the mining industry but also brings about severe environmental problems and security risks (tailings dam failure) in the mining regions.

With the recent push for sustainable development, the comprehensive utilization of IOTs has received increasing attention all over the world. Currently, the major utilization of IOTs includes land reclamation (Maiti et al. 2005), reextraction of iron or

other metals (Li et al. 2010; Sirkeci et al. 2006), and use as raw ingredients in producing infrastructure materials, backfilling materials, and fertilizers (Zhang et al. 2006; Zhu et al. 2011). The utilization of IOTs as a raw ingredient in the production of infrastructure materials is the focus of this paper. Past studies have reported several ways to utilize IOTs as additives in clinker (Wang and Wu 2000) and concrete (Zheng et al. 2010), as replacement of sand in concrete (Cai et al. 2009), as siliceous materials in ceramics (Liu et al. 2009; Das et al. 2000) and autoclaved aerated concrete (Li et al. 2011). The use of IOTs in the production of infrastructure materials promotes the sustainability of the mining industry and simultaneously enhances the greenness of the construction industry by reducing the demand for virgin materials.

Concrete is the most widely used infrastructure material on Earth, requiring tremendous amounts of raw materials that are often mined from natural landscapes. Worldwide, concrete production amounts to over 12 trillion kg per year (Van Oss and Padovani 2002) for new construction and repair. The production of each ton of concrete with a compressive strength of 35 MPa generates about 313 m<sup>3</sup> of CO<sub>2</sub> (Marceau et al. 2007), which is primarily associated with cement production. Globally, it is estimated that cement production alone is responsible for about 5% of anthropogenic CO<sub>2</sub> emissions (U.S. EPA 2000b). To promote the sustainability of concrete, extensive efforts have been put into screening suitable industrial byproducts to partially replace cement or aggregate in concrete (Badur and Chaudhary 2008; Ramazan and Rüstem 2006; Saikia and Brito 2012; Shi and Zheng 2007), thereby reducing the need for natural resources. Whereas the substitution of cement or aggregate by recycled materials in concrete improves material greenness, it is also necessary to ensure material durability in the use phase to attain true sustainability of concrete infrastructure (Keoleian et al. 2005b).

The durability of concrete is limited by its brittleness and crack formation at low tensile stresses, which lead to infrastructure deterioration problems (such as corrosion of reinforcing steel) and failures. To reduce the cracking tendency of concrete, fiber

<sup>1</sup>Graduate Student, State Key Laboratory of High-Efficient Mining and Safety of Metal Mines of Ministry of Education, Univ. of Science and Technology Beijing, Beijing 100083, China. E-mail: xiaoyan.hwang@gmail.com

<sup>2</sup>Graduate Student, Dept. of Civil and Environmental Engineering, Univ. of Michigan, Ann Arbor, MI 48109-2125. E-mail: ranade@umich.edu

<sup>3</sup>Professor, Dept. of Civil and Environmental Engineering, Univ. of Michigan, Ann Arbor, MI 48109-2125 (corresponding author). E-mail: vcli@umich.edu

Note. This manuscript was submitted on June 19, 2012; approved on August 28, 2012; published online on September 1, 2012. Discussion period open until December 1, 2013; separate discussions must be submitted for individual papers. This paper is part of the *Journal of Materials in Civil Engineering*, Vol. 25, No. 7, July 1, 2013. © ASCE, ISSN 0899-1561/2013/7-923-931/\$25.00.

reinforcement is typically introduced to alleviate its brittleness. Engineered cementitious composites (ECCs) is a unique class of high-performance fiber-reinforced cementitious composite that has a tensile strain capacity  $300\text{--}500\times$  greater than normal concrete and an intrinsically tight crack width (less than  $100\ \mu\text{m}$ ) under large deformation (Li 2003). Because of a high ductility and tight crack width, ECC exhibits excellent durability properties leading to prolonged service life and reduced maintenance frequency with respect to normal concrete (Li 2009b). The sustainability advantage of ECC infrastructure with respect to conventional concrete infrastructure has been demonstrated quantitatively in a bridge deck joint system through a lifecycle assessment of the economic and environmental performance (Keoleian et al. 2005a). Compared with conventional concrete joint systems, ECC joint system shows 30% savings in cost, 40% less energy consumption, and 39% less CO<sub>2</sub> emissions with respect to the entire bridge lifecycle (Keoleian et al. 2005a). Whereas ductile ECC demonstrates significant improvements in durability and infrastructure sustainability over normal concrete, it uses about  $2\text{--}3\times$  more cement, leaving room for further improvement in material greenness.

In a typical ECC mixture (ECC M45 in Wang and Li 2007), cement is a major contributor to environmental impacts among all ECC constituents (Fig. 1) and accounts for 48.2 and 81.6% of total primary energy consumption and carbon dioxide emissions, respectively. This is despite the use of a relatively large amount of fly ash ( $1.2\times$  that of cement). Therefore, reducing cement content can effectively lower the carbon and energy footprints of ECC.

In this paper, ground IOTs are investigated as potential replacement of cement in ECC mixture to enhance material greenness and maintain the high tensile ductility and tight crack width of ECC for long-term infrastructure sustainability. Experimental investigations focus on the characterization of ECC containing IOTs in terms of compressive strength, tensile ductility, and crack width. Material greenness is evaluated quantitatively by material sustainability indicators (MSIs) (Li et al. 2004). Results of the mechanical test and greenness evaluations of ECC with varying proportions of IOTs are documented in this paper.

## Experimental Program

### Material Design Considerations

The use of IOTs in the development of a ductile composite is guided by the micromechanics-based design theory of ECC (Li and Leung 1992; Lin and Li 1997; Li 1997). This theory has been successfully applied in the design of different kinds of ECC in

recent years (Kong et al. 2003; Wang and Li 2003; Kim et al. 2003; Wang and Li 2006). According to micromechanics-based design principles, the matrix fracture toughness of ECC has to be limited such that multiple cracking and strain hardening occurs before the tensile load reaches the fiber bridging capacity. Wang and Li (2007) found that partially replacing cement with mineral admixtures can effectively reduce the matrix fracture toughness, resulting in enhanced tensile ductility of ECC, as explained by the underlying micromechanics (Li 1997). The primary reason that underlies such successful approach is that the reactivity of mineral admixtures is less than that of cement. IOTs are ground natural rocks containing minerals with crystalline structure and are therefore expected to impart an inert property or low reactivity at ambient temperature when incorporated in cement-based materials. Hence, IOTs with reduced reactivity were adopted in this study to reduce the matrix fracture toughness for achieving desirable composite ductility guided by the micromechanics-based design principles of ECC.

A ground granulated blast furnace slag (BFS), instead of fly ash in ECC M45, was adopted as a mineral admixture in the mix design of green ECC containing IOTs. Both fly ash and BFS are industrial byproducts and are widely used as supplementary mineral admixtures in modern concrete or mortar. Typically, BFS with both cementitious and pozzolanic properties exhibits relatively higher reactivity than fly ash with only a pozzolanic property (Slag 2002). For maximizing the IOTs content in green ECC, commercially available ASTM-Grade 120 BFS (ASTM C989 2010) with relatively high reactivity (compared with fly ash) was strategically used to compensate for the potential loss of compressive strength of green ECC as a result of the reduced reactivity of the IOTs (compared with portland cement).

## Materials

The materials used for making green ECC in this study include IOTs, Type I ordinary portland cement (PC, ASTM C150/C150M 2012a), BFS, silica sand, polyvinyl alcohol (PVA) fiber, water, and a high-range water-reducing admixture (HRWRA). The BFS is ASTM-Grade 120 slag and has a Blaine fineness of  $550\ \text{m}^2/\text{kg}$ . The silica sand used in this study has a mean size of  $110\ \mu\text{m}$  and maximum size of  $250\ \mu\text{m}$ . All of the green ECC in this study used PVA fibers with diameters of  $39\ \mu\text{m}$  and lengths of 8 mm. In addition, these fibers have a thin oil coating (10–100 nm) of 1.2% by weight on the surface to control the interfacial bond properties. The nominal tensile strength, elastic modulus, and maximum elongation of the PVA fibers are 1620 MPa, 42.8 GPa, and 6%, respectively.

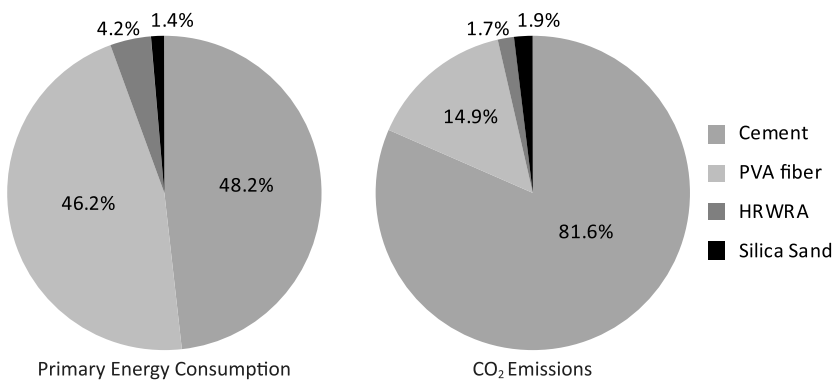


**Fig. 1.** Contributions of individual components in typical ECC M45 to MSIs (fly ash in ECC M45 is assumed to not contribute to carbon and energy footprints)

In this paper, IOTs were ground into fine powder with the particle size distributions given in Fig. 2 as determined using laser diffraction analysis (Kiattikomol et al. 2000). The mean size of the IOTs is approximately  $5\text{ }\mu\text{m}$  and 90% of particles are less than  $40\text{ }\mu\text{m}$ . The IOTs have a Blaine fineness of  $750\text{ m}^2/\text{kg}$ . For comparison, the typical particle size distribution of Type I portland cement is also included in Fig. 2. Chemical analysis (Table 1) indicates that IOTs are primarily comprised of silica with alumina and iron oxide. The mineral phases of IOTs were identified using the X-ray diffraction (XRD) technique, which showed that quartz is the major phase and amphibole and feldspar are minor phases (Fig. 3). Therefore, the finely ground IOTs can be regarded as ultrafine quartz powder to some extent. Recent research (Kronlof 1994; Benet and Benhassaine 1999; Lawrence et al. 2003) has found that quartz powder with a particle size of a few tens of microns or less exhibits the following three functions when incorporated in cement based materials: (1) increasing the packing density, (2) serving as nucleation sites to facilitate cement hydration, and (3) contributing to the long-term strength development through partial pozzolanic reactivity. Therefore, the ground IOTs used in this study may serve two purposes. The relatively large and inert

particles of IOTs compared with cement reduce the matrix fracture toughness and the ultrafine IOTs particles are expected to improve fiber/matrix interfacial properties as a result of these three effects noted previously, which contributes towards enhancing composite mechanical behavior.

Concentration of inorganic contaminants including As, Ba, Cd, Cr, Pb, Se, Ag, and Hg in the IOTs were examined to ensure that the IOTs were nonhazardous before using it in the production of a potential infrastructure material. These elements are identified by the U.S. EPA as inorganic analytes and their concentration should be measured to determine whether a waste is hazardous (U.S. EPA 2000b). As the IOTs used in this paper are the tailings separated from magnetite ore through only magnetic separation, indicating that there are no organic agents employed, there is no need to investigate the organic toxicity.

The inductively coupled plasma atomic emission spectroscopy (ICP-AES) technique was used to analyze the total concentration of As, Ba, Cd, Cr, Pb, Se, and Ag in IOTs. A fluorescence spectrophotometer was used to detect the total concentration of Hg. The test results are listed in Table 2 along with the regulatory limits specified by the U.S. EPA. The regulatory limits represent the maximum allowable concentration in a leachate obtained during the toxicity characteristic leaching procedure (TCLP), as prescribed by the U.S. EPA. If the waste is total solid, the U.S. EPA allows for an analysis of the total concentration of concerned chemicals and then dividing the total concentration measurements by 20 to obtain the theoretical maximum leachable concentration. The factor of 20 is derived from the 20:1 liquid-to-solid ratio employed in the TCLP. Both the total concentration and calculated maximum leachable concentration of IOTs are listed in Table 2. Table 2 indicates that all of the inorganic contaminants exhibit concentrations well below the regulatory limits; therefore, the IOTs used in this study can be considered as nonhazardous industrial waste.

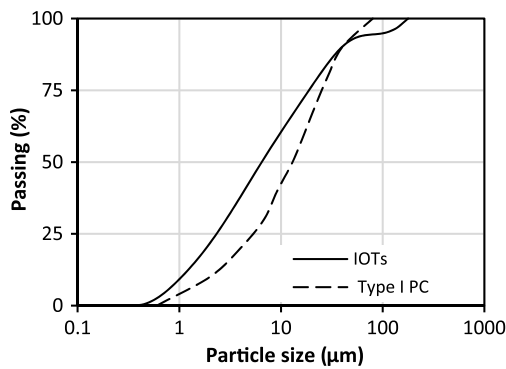


**Fig. 2.** Particle size distribution of IOTs and cement; data for portland cement adapted from Kiattikomol et al. (2000)

**Table 1.** Chemical Composition of Iron Ore Tailings in Units of Weight Percent

SiO <sub>2</sub>	CaO	Al <sub>2</sub> O <sub>3</sub>	MgO	Fe <sub>2</sub> O <sub>3</sub>	Na <sub>2</sub> O	K <sub>2</sub> O	SO <sub>3</sub>	Loss
69.52	4.14	7.44	3.72	8.13	1.38	1.97	0.03	2.51

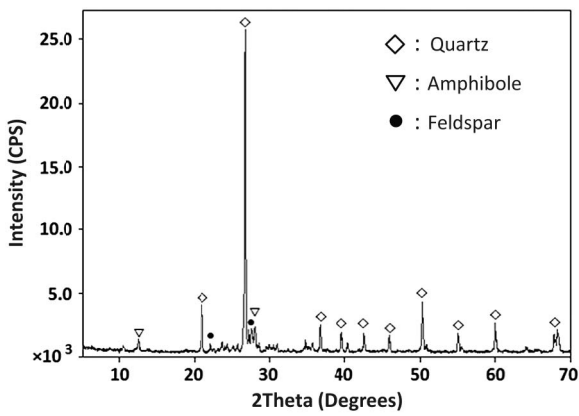


**Fig. 3.** X-ray diffraction pattern of IOTs

### Mixture Proportions

Table 3 shows the mixture proportions of all the ECCs investigated in this study. Using ECC M45 as a template for the new mixtures, silica sand/powder (cement, IOTs, and BFS) and water/powder ratios were set at 0.36 and 0.27, respectively. The HRWRA content was varied between different mixtures to achieve the viscosity required for homogenous fiber dispersion. Viscosity was indirectly measured using the Marsh cone flow test and the targeted flow time of the fresh matrix mixture (ECC without the fiber) was 25–35 s, as recommended by Li (2009a). The fiber volume fraction was fixed at 2% for all of the mixes. The mixtures M1–3 were designed to investigate the effect of different amounts of cement replacement by IOT on the mechanical properties of ECC. In the control mixture

**Table 2.** IOTs Contaminant Concerns

Contaminant	Regulatory level (mg/L)	Concentration of contaminants in IOTs	
		Total concentration (mg/kg)	Maximum leachable concentration (mg/L)
As	5	N/A	N/A
Ba	100	0.97	0.05
Cd	1	0.05	0.0025
Cr	5	1.56	0.08
Pb	5	1.28	0.06
Hg	0.2	0.04	0.002
Se	1	N/A	N/A
Ag	5	0.37	0.02

Note: N/A = not available.

**Table 3.** Mixture Proportions of ECCs

Mix ID	Cement		IOTs		BFS		Silica sand	HRWRA /power	Matrix
	Cement replacement (%)	Weight proportion (%)	kg/m <sup>3</sup>	Weight proportion (%)	kg/m <sup>3</sup>	Weight proportion (%)	kg/m <sup>3</sup>		
M1	0	1.0	593.3	0	0	1.2	711.9	469.9	0.42
M2	40	0.6	350.2	0.4	233.5	1.2	700.5	462.3	0.46
M3	80	0.2	117.2	0.8	468.6	1.2	703.3	464.1	0.44
M4	—	0.6	348.9	1.2	697.9	0.4	232.6	460.6	0.48
M5	—	0.4	254.7	1.2	764.1	0.4	254.7	458.5	0.45

M1, the ratio of BFS to cement was set at 1.2, adopted from the fly ash to cement ratio in typical ECC M45 (M1 and M45 have the same mix design, except that the fly ash in M45 is replaced by BFS). The cement was then replaced by IOTs at two different levels (40 and 80%) in M2 and M3. Among mixtures M1–3, M2 shows the highest tensile strain capacity, and therefore increased amounts of IOTs are used to replace BFS in mixture M4 for maximizing the material greenness. Finally, the possibility of further lowering the cement content in mixture M4 was explored in mixture M5. The overall objective of this mixture design strategy was to improve the material greenness by reducing the cement content and increasing the fraction of IOTs, and maintain the established tensile ductility of ECC M45 as much as possible.

### Specimen Preparation and Testing

All of the solid ingredients were first mixed without water for approximately 2–3 min at a low speed in a 3-L Hobart mixer. Water and HRWRA were then added and mixed for 1 min at a low speed and for another 2 min at a high speed. After the matrix ingredients were thoroughly mixed to achieve a fresh flowable state, the Marsh cone flow time of the matrix was measured to ensure that the viscosity was within the desired range for achieving good fiber dispersion. Finally, fibers were added at a low speed and then mixed with the matrix mixture at a high speed for 2 min. The mixture was then cast into molds on a vibration table with a moderate vibration rate. All of the specimens were demolded after 24 h and then cured in a plastic bag at a room temperature of approximately  $23 \pm 3^\circ\text{C}$  until the day of testing.

The mechanical properties for all of the ECC specimens were tested at the age of 28 days. For each mixture, three 50-mm cube specimens were prepared for the uniaxial compression test, and three dogbone specimens were prepared for the uniaxial tensile test. The geometry of dogbone specimen can be found in Ranade et al. (2011). The uniaxial tensile test was conducted on a displacement controlled test system that had a loading rate of 0.5 mm/min. Two linear variable differential transformers (LVDTs) were attached on the specimen with a gauge length of approximately 100 mm to measure the tensile extension. The residual crack width in dogbone specimens was measured after unloading using a portable microscope as described in Li and Li (2009).

To gain further insights into the effects of binder modification on the tensile response of ECC, the matrix fracture toughness of all mixtures was tested in accordance with ASTM E399 (ASTM 2012b). Although this standard, based on the linear elastic fracture mechanics (LEFM) approach, is meant for metal testing, it is applicable for testing brittle mortar matrices, attributable to small-scale yielding near the crack tip (Li et al. 1995). Four notched beam specimens measuring 305 mm in length, 76 mm in height, and 38 mm in thickness were cast without adding fibers. The span length is 254 mm and the notch depth to beam height ratio was 0.4.

## Experimental Results and Discussion

### Uniaxial Tensile Performance

Table 4 summarizes the uniaxial tensile test results in terms of first cracking strength, ultimate tensile strength, tensile strain capacity, and residual crack width of mixtures M1–5 at the age of 28 days. Each data is an average of three test results. Fig. 4 presents complete tensile stress-strain curves of these composites. All of the mixtures M1–5 exhibit strain-hardening behavior with tensile strain capacities ranging from 1.8–3.3%, approximately 180–300× the ductility of normal concrete. The first cracking strength and ultimate tensile strength of mixtures M1–5 vary from 3.8–5.1 MPa and from 5.1–6.1 MPa, respectively, which are slightly greater than those of typical ECC M45 (Wang and Li 2007).

According to the micromechanics-based design theory of ECC, there are two necessary conditions that must be satisfied for achieving strain hardening (Li and Leung 1992; Li 1997). The first condition requires that the fiber-bridging capacity ( $\sigma_0$ ) must be greater than the cracking strength ( $\sigma_{cr}$ ) on any given crack plane. The second condition requires that the crack tip toughness ( $J_{tip}$ ) be less than the complementary energy ( $J'_b$ ) of fiber-bridging. Large margins between  $\sigma_0$  and  $\sigma_{cr}$ , and between  $J_{tip}$  and  $J'_b$  are both desirable for increasing the potential for saturated multiple cracking, resulting in consistently high tensile ductility of ECC (Kanda and Li 2006). Reducing the  $J_{tip}$  value can be achieved by reducing the matrix fracture toughness and increasing the  $\sigma_0$  value can be achieved by controlling the fiber/matrix interfacial properties.

For mixtures M1–3, as the replacement of cement with IOTs increases, the tensile strain capacity first increases from M1—M2 and then decreases from M2—M3. However, the tensile strain capacity of mixture M3 (the least of them all) still exceeds 2% at cement contents as little as 117.2 kg/cm<sup>3</sup>, which accounts for only approximately 7% of the total solid matrix materials. This cement content is even less than that typically used in normal concrete that has a compressive strength greater than 30 MPa. The improvement in the tensile strain capacity of mixture M2 as compared with M1 can be attributed to the reduction of the matrix fracture toughness (Fig. 5) because of the replacement of cement by IOTs. The reduction of matrix fracture toughness is primarily caused by the

**Table 4.** Tensile Properties of ECCs at 28 Days

Mix ID	First cracking strength (MPa)	Tensile strength (MPa)	Tensile strain (%)	Approximate residual crack width (μm)
M1	5.1 ± 0.6	6.1 ± 0.2	1.8 ± 0.7	36
M2	4.4 ± 0.2	6.0 ± 0.2	3.1 ± 0.5	31
M3	4.7 ± 0.4	5.3 ± 0.3	2.3 ± 0.7	23
M4	3.9 ± 0.2	5.5 ± 0.1	3.3 ± 0.1	27
M5	3.8 ± 0.1	5.1 ± 0.5	3.3 ± 0.5	30

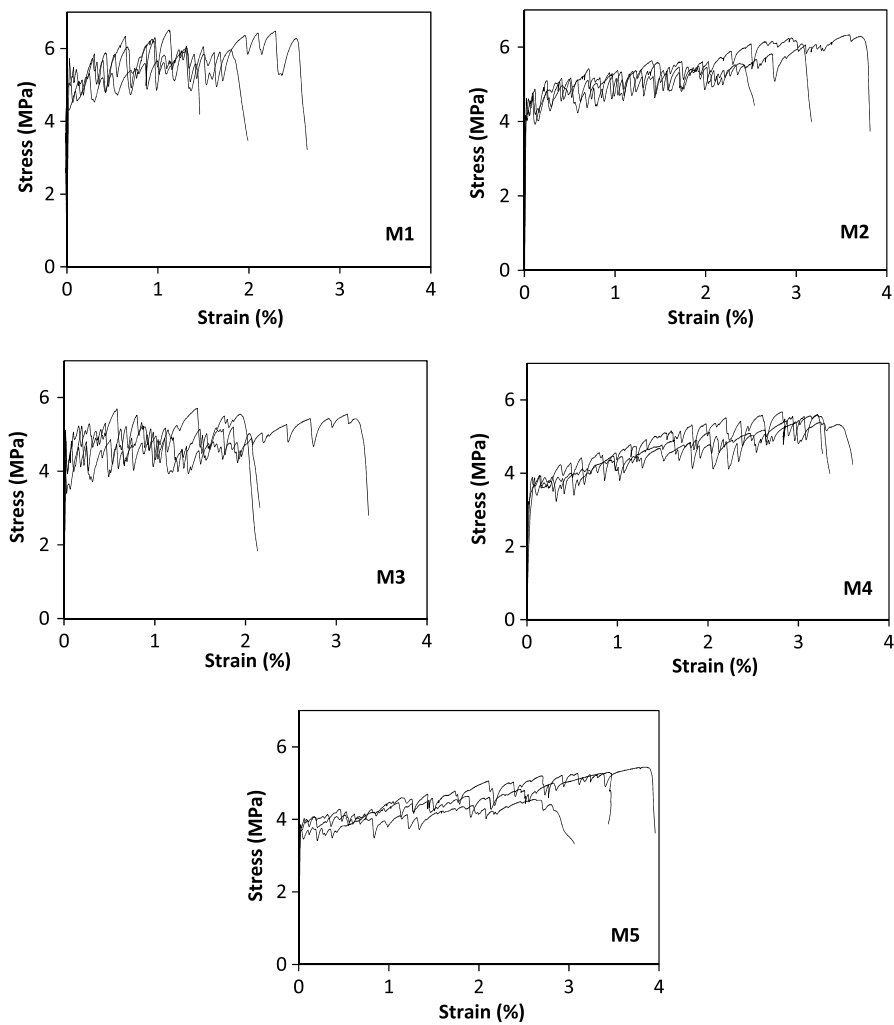


**Fig. 4.** Tensile stress-strain curves of ECC mixtures at 28 days (three repeated tests were conducted for each mix design)

relatively inert IOT particles with crystalline structure as the bond between IOT and cementitious particles (cement or BFS) is weaker than that between the particles of cementitious materials. However, excessive cement replacement by IOTs lowers the fiber-bridging capacity  $\sigma_0$  as indicated by the decrease in the ultimate tensile strength of mixture M3 (Table 4), which reduces the margin between  $\sigma_{cr}$  and  $\sigma_0$ , leading to a reduction and less consistency

in tensile ductility. The decrease in fiber bridging capacity in M3 compared with M2 can be attributed to a weaker fiber/matrix interfacial bond caused by the reduction of strong hydration products. To confirm the influence of IOTs replacement with cement on the fiber/matrix interface properties in terms of frictional and chemical bonds, a micromechanical study through a single-fiber pullout test is further needed. Nevertheless, the current study successfully demonstrates the feasibility of green ECC with consistently high tensile ductility by controlling the amount of IOTs that replace the cement.

Compared with mixture M2, mixture M4 shows a slight increase in tensile ductility with improved consistency in mechanical properties. With a moderate cement content of  $348.9 \text{ kg/m}^3$ , the high replacement of BFS by IOTs in M4 improves its tensile ductility. This is attributable to further reduction of matrix fracture toughness (Fig. 5) in M4. The lesser cement content in M5 compared with M4 does not cause a significant reduction in average tensile ductility; however, it shows a relatively larger variation. In spite of the high usage of IOTs in M5 that has a cement content of only  $254.7 \text{ kg/m}^3$ , it still achieves a tensile ductility of at least 2.7%. As the decrease in cement content in mixture M5 negatively influences the tensile performance, further reduction of cement content was not explored in this paper. From the test results of mixtures M4–5, it can be concluded that highly ductile BFS-based ECC-containing IOT as much as  $697.9\text{--}764.1 \text{ kg/m}^3$ , which

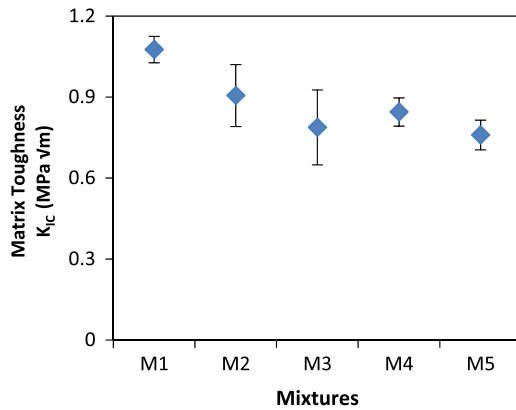


**Fig. 5.** Matrix fracture toughness of mixtures M1–5

constitutes more than 50% of the total solid powder materials of the ECC matrix, can be achieved.

The first cracking strength under tension of mixtures M1–3 first decreases and then increases. From Irwin's fracture criterion, the matrix cracking strength is influenced by both matrix fracture toughness and the largest flaw size (Li et al. 1995). The test results (Fig. 5) indicate that increasing replacement of cement by IOTs from M1—M3 causes a reduction in the matrix fracture toughness. The first crack strength is proportional to the matrix fracture toughness and is therefore expected to reduce with increasing cement replacement from M1—M3, provided that the maximum flaw size is similar in these composites. Hence, the observed increase in first crack strength from M2—M3 might be caused by the reduction in maximum flaw size. This is further supported by the Marsh cone flow test as the flow time of the fresh matrix mixture of M3 is less than that of mixtures M1–2 (see Table 3). The reduced flow time of M3 indicates lower viscosity and higher flowability, thus resulting in smaller maximum flaw size. As a result, the first cracking strength of mixture M3 is higher than M2 in spite of the lower matrix fracture toughness of M3 compared with M2. Both mixtures M4 and M5 exhibit reduced first crack strength as the content of cementitious material decreases, which is consistent with the trend of matrix fracture toughness (see Fig. 5). Thus, incorporation of IOT in ECC generally reduces the first cracking strength of ECC as a result of the decreasing matrix fracture toughness; however, the ECC M5 with the highest IOTs content of  $764.1 \text{ kg/m}^3$  still achieves a first cracking strength of 3.8 MPa.

The average residual crack width of mixtures M1–5 ranges from 23–36  $\mu\text{m}$  (Table 4). Fig. 6 shows the crack pattern of mixture M5 after unloading. It clearly shows the multiple-cracking behavior of green ECC with a narrow crack spacing of 2–3 mm. Because of the elastic recovery of the fibers bridging the matrix cracks, the residual crack width measured after unloading is less than that under loaded state. The average crack width under load is typically about twice that of the average residual crack width (Yang et al. 2007). Accordingly, the average crack width under load of mixtures M1–5 is approximately 46–72  $\mu\text{m}$ . Such a tight crack width implies superior durability of green ECC over cracked brittle concrete with crack width at the scale of several hundred microns to a few millimeters.

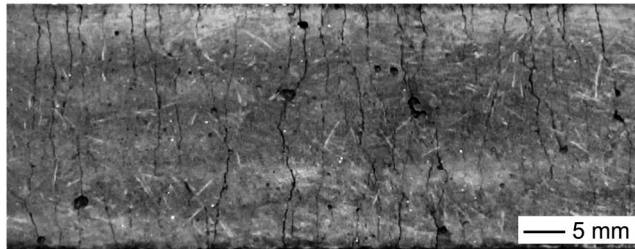


**Fig. 6.** Crack pattern of ECC M5

### Material Greenness Evaluation

Material greenness of ECC is quantified by MSIs, which account for the primary energy consumption and carbon dioxide emissions generated in the production of all the material components per unit volume of composites. The MSI source for BFS is Marceau and VanGeem (2003). All other data for MSIs calculation is originally from the sources listed in Table 5 compiled by Kendall et al. (2008). In the case of IOTs, the only significant contribution to MSI comes from the process of grinding larger IOT particles into the powder form that was used in this paper. However, there is no data available in the literature for primary energy consumption and carbon dioxide emissions during the grinding process. In this paper, the MSIs of IOTs per unit mass are conservatively estimated to be the same as commercial BFS. This estimation is made based on a study on the grindability of high-quartz IOTs in comparison to blast furnace slag (Huang et al. 2010). The MSI of ECC is computed by aggregating the MSI of IOTs and other components used per unit volume of ECC, which forms an effective and convenient tool to compare the material environmental impact of ECC comprised of different component materials.

Fig. 7 is a plot of the MSIs of ECC M1–5 against tensile strain capacity. Contrary to common opinion, Fig. 7 shows that reducing the MSIs does not necessarily compromise the tensile performance of ECC. The tensile ductility of green ECC-containing IOTs is maintained or even improved through the application of the micro-mechanics theory for designing these materials. MSIs of mixtures M1–5 and normal concrete (35 MPa) (see Fig. 8) are normalized with respect to typical ECC M45 for comparison purposes. The mixture M1 shows higher MSIs than ECC M45. This is reasonable as BFS (which replaces fly ash that is typically used in ECC M45) used in mixture M1 consumes additional energy for grinding as compared with fly ash which does not require extensive processing. Mixtures M2–5, which contain IOTs, demonstrate 10–32% less

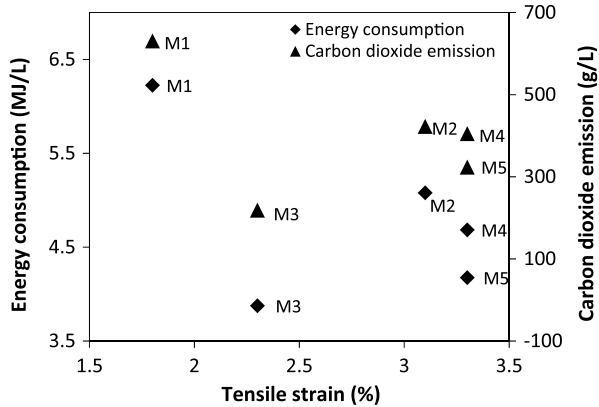


**Fig. 7.** MSIs of ECC M1–5 as a function of tensile strain

**Table 5.** Sources for MSIs

Material	Source of MSI information
Cement	Portland Cement Association (Nisbet et al. 2002) and Ecobilan (Ecobilan 2001) cement data
Sand	Portland Cement Association (Nisbet et al. 2002), adjusted with electricity and fuel (EPA 2000a) from Ecobilan (2001) and equipment emissions from U. S. EPA's (2000a) Nonroad
Polyvinyl alcohol fiber	Industry source and polyethylene data from Association of Plastic Manufacturers in Europe (Bousted 1999)
High-rate water reducer	Acrylonitrile MSIs dataset from the Association of European Plastic Manufacturers (Bousted 2005) used as a surrogate (this data set is considered a lower bound for polycarboxylated polymer MSIs)
admixture, polycarboxylated polymer-based	

Note: Data adapted from Kendall et al. (2008).

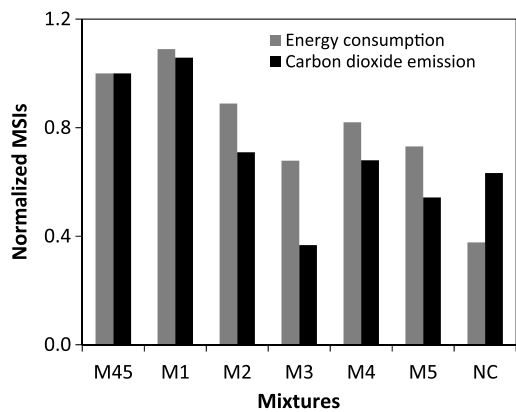


**Fig. 8.** Comparisons of MSIs between ECC M45, mixtures M1–5, and normal concrete (NC)

energy consumption and 29–63% less carbon dioxide emissions with respect to ECC M45, resulting in greener ECC materials.

Compared with normal concrete, ECC mixtures M3 and M5 generate a lesser amount of carbon dioxide, whereas all of the ECC mixtures M1–5 still consume more energy than normal concrete. This is not surprising because a large amount of energy consumed in the production of ECC raw materials comes from the highly energy-intensive PVA fibers (Fig. 1). Even though the content of PVA fibers is optimized with a volume fraction of only 2%, the associated primary energy consumption is approximately 46% of the total energy consumption of all the ECC constituents. It is necessary to reduce the environmental impact of fiber reinforcement in the future for achieving further improvements in material greenness. Except for the greater energy consumption of green ECC than normal concrete, green ECC with cementitious materials (cement and BFS) replaced by IOT exhibit improved environmental performance as compared with typical ECC M45 and normal concrete. This is in addition to the large amount of industrial waste recycled into the green ECC. Thus, a low environmental impact (measured by MSIs) and high tensile ductility of green ECC can be simultaneously obtained through the incorporation of IOTs.

### Compressive Strength

Fig. 9 summarizes the average compressive strength test results of mixtures M1–5 at 28 days. Each data is an average of three test results. All of the ECC mixtures exhibit a compressive strength that is greater than 46 MPa. For the mixtures M1–3, replacement of the cement by IOTs reduces the compressive strength. This is a result

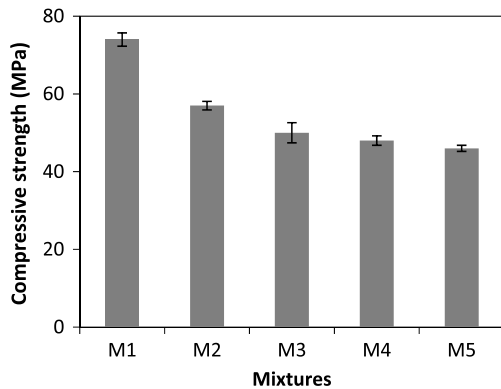


**Fig. 9.** Compressive strength of mixtures M1–5 at an age of 28 days

of the decreasing amount of hydration products, which is attributable to the reduction of cement content. The compressive strength of mixture M3, which contains cement as little as 117.2 kg/m<sup>3</sup>, reaches approximately 50 MPa (the same as high-strength concretes). The moderately high compressive strength of ECC M3 is likely attributable to the incorporation of highly reactive BFS and IOTs with a large amount of ultrafine particles with diameters under 10 microns. These ultrafine particles in IOTs not only serve as filler materials in elevating the compactness of the matrix but also as nucleation sites in accelerating the rate of cement hydration (Kronlof 1994; Lawrence et al. 2003). Both effects are beneficial for maintaining the compressive properties of ECC with a high content of IOTs. In addition, ultrafine particles in IOTs may exhibit partial pozzolanic activity beyond the age of 28 days (Guettala and Mezghiche 2011), which is favorable for long-term strength development.

Comparing mixture M4 with M2, the replacement of more reactive BFS by relatively inert IOTs causes a reduction in compressive strength as expected. The IOT and BFS content is further increased in M5 to reduce cement in M4, bringing the IOT/all-solid powder materials ratio up to 60%. In spite of such a high IOT content, the compressive strength of the mixture M5 is 46 MPa. Overall, the increase in the IOTs content leads to a decrease in compressive strength when the replacement ratio of cementitious materials by IOTs exceeds 40% as studied in this paper; nevertheless, the compressive strength of green ECC mixtures M2–5 that contain IOTs is similar or close to that of high-strength concrete.

### Conclusions

This paper demonstrates the feasibility of incorporating iron ore tailings to develop green ECC, which not only maintains high-tensile ductility characteristics but also greatly improves material sustainability. Based on the results obtained, the following conclusions can be drawn:

- Green ECC exhibits a tensile strain capacity of 2.3–3.3% and tensile strength greater than 5.1 MPa in spite of large replacements of cement by IOTs. The cement content of green ECC is reduced to 117.2–350.2 kg/m<sup>3</sup>, which is close to or even less than the cement content in ordinary concrete.
- The replacement of cement or BFS by less reactive IOTs in ECC reduces the matrix fracture toughness. The reduction in matrix toughness is conducive to achieving improved strain-hardening and multiple cracking behavior of green ECC. To fully understand the influence of IOTs on the overall mechanical performance of green ECC, further research on the micrometer scale is needed to investigate the influence of IOTs on the fiber/matrix interface properties through single-fiber pullout tests.
- Increasing the replacement of cement or BFS beyond 40% replacement ratio reduces the compressive strength of ECC. However, with a cement content of only 117.2 kg/m<sup>3</sup>, the 28-days compressive strength of ECC that contain ultrafine IOTs can still reach 50 MPa, which can fulfill the strength requirements of many applications.
- MSI analysis shows that the addition of IOTs in the production of ECC leads to enhancement of material greenness through reduction in the primary energy consumption and carbon dioxide emissions. In this paper, the green ECC designed with a tensile ductility of 2.3–3.3% and compressive strength of 46–57 MPa demonstrate 10–32% less energy consumption and 29–63% less carbon dioxide emissions with respect to typical ECC M45.

The newly developed green ECC is expected to improve infrastructure sustainability through a combination of green material

constituents and high-tensile ductility. In addition, the successful utilization of IOT in the development of high-performance infrastructure materials provides great benefits in the sustainable development of the mining industry.

## Acknowledgments

Support from the National Science Foundation (CMMI 1030159) to the University of Michigan is gratefully acknowledged. Xiaoyan Huang is supported by a grant from the Chinese Scholarship Council as a visiting scholar at the University of Michigan. The authors would like to acknowledge Lafarge (cement), U.S. Silica (silica sand), W. R. Grace (HRWRA), Kuraray (PVA fiber), and Shouyun (iron ore tailings) for material supplies. The authors would also like to thank Li Hong of the University of Science and Technology Beijing for XRD tests and Hu Gang of the Institute of Tibetan Plate Research, Chinese Academy of Sciences, for his assistance in particle size distribution tests.

## References

- ASTM. (2010). "Standard specification for slag cement for use in concrete and mortars." *C989*, West Conshohocken, PA.
- ASTM. (2012a). "Standard specification for Portland cement." *C150/C150M*, West Conshohocken, PA.
- ASTM. (2012b). "Standard test method for linear-elastic plane-strain fracture toughness K Ic of metallic materials." *E399-12*, West Conshohocken, PA.
- Badur, S., and Rubina, B. (2008). "Utilization of hazardous wastes and by-products as a green concrete material through s/s process: A review." *Rev. Adv. Mater. Sci.*, 17(1–2), 42–61.
- Benezet, J. C., and Benhassaine, A. (1999). "The influence of particle size on the pozzolanic reactivity of quartz powder." *Powder Technol.*, 103(1), 26–29.
- Bouston, I. (1999). "High density polyethylene." Eco-profiles of Plastics and Related Intermediates. Brussels, Association of Plastics Manufacturers in Europe.
- Bouston, I. (2005). "Acrylonitrile." Eco-Profiles for the European Plastics Industry. Brussels, Association of European Plastic Manufacturers.
- Cai, J.-W., Zhang, S.-B., Hou, G.-X., and Wang, C.-M. (2009). "Effects of ferrous mill tailings as aggregates on workability and strength of concrete." *J. Wuhan Univ. Technol.*, 31(7), 104–107 (in Chinese).
- Das, S. K., Kumar, S., and Ramachandrarao, P. (2000). "Exploitation of iron ore tailing for the development of ceramic tiles." *Waste Manage.*, 20(8), 725–729.
- Ecobilan-PricewaterhouseCoopers. (2001). *TEAM/DEAM databases*, Ecobilan, Rockville, MD.
- Guettala, S., and Mezghiche, B. (2011). "Compressive strength and hydration with age of cement pastes containing dune sand powder." *Constr. Build. Mater.*, 25(3), 1263–1269.
- Huang, X.-Y., Ni, W., Zhu, L.-P., and Wang, Z.-J. (2010). "Grinding characteristic of Qidashan iron tailings." *J. Univ. Sci. Technol. Beijing*, 32(10), 1253–1257 (in Chinese).
- Kanda, T., and Li, V. C. (2006). "Practical design criteria for saturated pseudo strain hardening behavior in ECC." *J. Adv. Concr. Technol.*, 4(1), 59–72.
- Kendall, A., Keoleian, G. A., and Lepech, M. (2008). "Material design for sustainability through life cycle modeling of engineered cementitious composites." *Mater. Struct.*, 41(6), 1117–1131.
- Keoleian, G. A., et al. (2005a). "Life-cycle cost model for evaluating the sustainability of bridge decks." *Proc., Int. Workshop on Life-Cycle Cost Analysis and Design of Civil Infrastructure Systems*, ASCE, Reston, VA, 143–150.
- Keoleian, G. A., et al. (2005b). "Life cycle modeling of concrete bridge design: Comparison of ECC link slabs and conventional steel expansion joints." *J. Infrastruct. Syst.*, 11(1), 51–60.
- Kiatikomol, K., Jaturapitakkul, C., and Tangpagasit, J. (2000). "Effect of insoluble residue on properties of portland cement." *Cement Concr. Res.*, 30(8), 1209–1214.
- Kim, Y. Y., Kong, H. J., and Li, V. C. (2003). "Design of engineered cementitious composite suitable for wet-mix shotcreting." *ACI Mater. J.*, 100(6), 511–518.
- Kong, H. J., Bike, S., and Li, V. C. (2003). "Development of a self-consolidating engineered cementitious composite employing electrosteric dispersion/stabilization." *Cement Concr. Compos.*, 25(3), 301–309.
- Kronlof, A. (1994). "Effect of very fine aggregate on concrete strength." *Mater. Struct.*, 27(1), 15–25.
- Lawrence, P., Cyr, M., and Ringot, E. (2003). "Mineral admixtures in mortars, effect of inert materials on short-term hydration." *Cement Concr. Res.*, 33(12), 1939–1947.
- Li, C., Sun, H.-H., Bai, J., and Li, L.-T. (2010). "Innovative methodology for comprehensive utilization of iron ore tailings: Part 1. The recovery of iron from iron ore tailings using magnetic separation after magnetizing roasting." *J. Hazard. Mater.*, 174(1–3), 71–77.
- Li, D.-Z., Ni, W., Zhang, J.-W., Wu, H., and Zhang, Y.-Y. (2011). "Phase transformation of iron ore tailings during autoclaved curing." *J. Chin. Ceram. Soc.*, 39(4), 708–804.
- Li, M. (2009a). "Multi-scale design for durable repair of concrete structures." Ph.D. thesis, Univ. of Michigan, Ann Arbor, MI.
- Li, M., and Li, V. C. (2009). "Influence of material ductility on the performance of concrete repair." *ACI Mater. J.*, 106(5), 419–428.
- Li, V. C. (2009b). "Driving infrastructure sustainability with strain hardening cementitious composites." *Proc., Int. Conf. on Advanced Concrete Materials*, Advanced Civil Engineering—Materials Research Laboratory, Univ. of Michigan, Ann Arbor, MI, 181–192.
- Li, V. C. (1997). "Engineered cementitious composites—Tailored composites through micromechanical modeling." *Fiber reinforced concrete: Present and the future*, N. Banthia, A. Bentur, and A. Mufti, eds., Canadian Society for Civil Engineering, Montréal, 64–97.
- Li, V. C. (2003). "On engineered cementitious composites (ECC)—A review of the material and its applications." *J. Adv. Concr. Technol.*, 1(3), 215–230.
- Li, V. C., Lepech, M., Wang, S., Weimann, M., and Keoleian, G. (2004). "Development of green ECC for sustainable infrastructure system." *Proc., Int. Workshop on Sustainable Development and Concrete Technology*, Iowa State Univ., Ames, IA, 181–192.
- Li, V. C., and Leung, C. K. Y. (1992). "Steady state and multiple cracking of short random fiber composites." *J. Eng. Mech.*, 118(11), 2246–2264.
- Li, V. C., Mishra, D. K., and Wu, H. C. (1995). "Matrix design for pseudo strain-hardening fiber reinforced cementitious composites." *RILEM J. Mater. Struct.*, 28(10), 586–595.
- Lin, Z., and Li, V. C. (1997). "Crack bridging in fiber reinforced cementitious composites with slip-hardening interfaces." *J. Mech. Phys. Solids*, 45(5), 763–787.
- Liu, M., Xu, L.-H., Zhang, X.-M., Hao, H.-S., and Di, Y.-P. (2009). "Preparation of eco-friendly composite ceramic from iron ore tailings." *Mater. Sci. Forum*, 803(610), 281–284.
- Maiti, S. K., Nandhini, S., and Das, M. (2005). "Accumulation of metals by naturally growing herbaceous and tree species in iron ore tailings." *Int. J. Environ. Stud.*, 62(5), 595–603.
- Marceau, M. L., Nisbet, M. A., and VanGeem, M. G. (2007). "Life cycle inventory of portland cement concrete." *SN3011*, Portland Cement Association, Skokie, IL.
- Marceau, M. L., and VanGeem, M. G. (2003). "Life cycle inventory of slag cement manufacturing process." *Construction Technology Laboratories (CTL) Project No. 312012*, Slag Cement Association, Skokie, IL.
- Meng, Y.-H., Ni, W., and Zhang, Y. (2011). "Current state of ore tailings reusing and its future development in China." *China Mine Eng.*, 39(5), 4–9 (in Chinese).
- Ministry of Industry, and Information Technology of the People's Republic of China (MIITPRC). (2013). "Plan on the comprehensive utilization of metal ore tailings for 2010–2015." (<http://www.miit.gov.cn/n11293472/n11293832/n12843926/13158991.html>) (Apr. 14, 2013) (in Chinese).

- Nisbet, M. A., Marceau, M. L., and VanGeem, M. G. (2002). *Life cycle inventory of portland cement manufacture (An appendix to environmental life cycle inventory of Portland cement concrete)*, Portland Cement Association, Skokie, IL.
- Ramazan, D., and Rüstem, G. (2006). "Production of high strength concrete by use of industrial by-products." *Build. Environ.*, 41(8), 1124–1127.
- Ranade, R., Stults, M. D., Li, V. C., Rushing, T. S., Roth, J., and Heard, W. F. (2011). "Development of high strength high ductility concrete." *Proc., 2nd Int. RILEM Conf. on Strain Hardening Cementitious Composites*, RILEM Publications, Bagneux, France, 1–8.
- Saikia, N., and Brito, J. (2012). "Use of plastic waste as aggregate in cement mortar and concrete preparation: A review." *Constr. Build. Mater.*, 34(1), 385–401.
- Shi, C.-J., and Zheng, K.-R. (2007). "A review on the use of waste glasses in the production of cement and concrete." *Resour. Conserv. Recycl.*, 52(2), 234–247.
- Sirkeci, A. A., Gul, A., and Bulut, G. (2006). "Recovery of Co, Ni, and Cu from the tailings of divrigi iron ore concentrator." *Miner. Process. Extr. Metall. Rev.*, 27(2), 131–141.
- Slag Cement Association. (2002). "Slag cement and fly ash." *Rep. 11*, Slag Cement Association, Woodstock, GA.
- United States Environmental Protection Agency (U.S. EPA). (2000a). "NONROAD." Ann Arbor, MI.
- United States Environmental Protection Agency (U.S. EPA). (2000b). "Sources of dioxin-like compounds in the United States. Draft exposure and human health reassessment of 2, 3, 7, 8-tetrachlorodibenzo-p-dioxin (TCDD) and related compounds." *Rep. No. EPA/600/p-00/001Bb*, Washington, DC.
- Van Oss, H. G., and Padovani, A. C. (2002). "Cement technology." *J. Ind. Ecol.*, 6(1), 89–105.
- Wang, J.-Z., and Wu, C. (2000). "Effect of energy saving and formation of portland cement clinker using iron-tailings as raw materials." *J. Shenyang Arch. Civ. Eng. Inst.*, 16(2), 112–114 (in Chinese).
- Wang, S., and Li, V. C. (2003). "Materials design of lightweight PVA-ECC." *Proc., 4th Int. RILEM Workshop on High Performance Fiber Reinforced Cement Composites (HPFRCC 4)*, RILEM Publications, Bagneux, France, 379–390.
- Wang, S., and Li, V. C. (2006). "High-early-strength engineered cementitious composites." *ACI Mater. J.*, 103(2), 97–105.
- Wang, S., and Li, V. C. (2007). "Engineered cementitious composites with high-volume fly ash." *ACI Mater. J.*, 104(3), 233–241.
- Yang, E. H., Yang, Y., and Li, V. C. (2007). "Use of high volumes of fly ash to improve ECC mechanical properties and material greenness." *ACI Mater. J.*, 104(6), 620–628.
- Zhang, S., et al. (2006). "Current situation and comprehensive utilization of iron ore tailing resources." *J. Min. Sci.*, 42(4), 403–408.
- Zheng, Y.-C., Ni, W., Xu, L., Li, D.-Z., and Yang, J.-H. (2010). "Mechanochemical activation of iron ore tailings and preparation of high-strength construction materials." *J. Univ. Sci. Technol. Beijing*, 32(4), 504–507 (in Chinese).
- Zhu, L.-P., Ni, W., Huang, D., Hui, M., and Gao, S.-J. (2011). "Whole-tailings backfilling materials with fly ash." *J. Univ. Sci. Technol. Beijing*, 33(10), 1190–1196 (in Chinese).